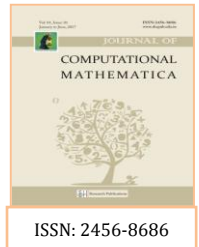




Journal of Computational Mathematica

Journal homepage: www.shcpub.edu.in



ISSN: 2456-8686

On Construction of stability methods for IVGTT glucose-insulin model with two distributed delays

¹P. Krishnapriya, and ²M. Pitchaimani

Received on 14 Feb 2017, Accepted on 08 April 2017

ABSTRACT. The intravenous glucose tolerance test (IVGTT) has been considered as the most accurate method to determine the insulin sensitivity and glucose effectiveness. In this paper, we present the extensions of various stability theorems for IVGTT model with two distributed delays. Sensitivity analysis for glucose insulin IVGTT system suggests that the parameter value has a major impact on the model dynamics. In addition, the numerical calculations in this paper is fully incorporated with initial conditions, which is natural and more appropriate in IVGTT model.

Key words: Glucose - Insulin - Dynamical model - Distributed delays - State Systems.

Mathematics Subject Classification (2010): 37B25, 93C10, 93C23.

1. INTRODUCTION

Several IVGTT models have been proposed and some are widely used [1–6]. All these models incorporate insulin secretion delay implicitly in ordinary differential equation (ODE) model by using compartment-split technique or explicitly in delay differential equation (DDE) models. In the procedure of IVGTT, overnight fast is required for the subject, and then the subject is given a bolus of glucose infusion intravenously. Due to its relatively simple structure and to its great clinical importance, the glucose/insulin system has been the object of repeated mathematical modeling attempts [7–25]. However none of the above work has discussed the two distributed delay model for IVGTT glucose-insulin secretion. Many authors in the last decades proposed and studied different models for the glucose-insulin homeostasis [1,2,4,6,26–28]. The models here adopted to estimate the time course of the plasma insulin concentration are families of distributed delay models with single and double kernel [4]. Such models allow to couple the dynamics of both glucose and insulin kinetics in a unique extended system, whose solutions have been proven to be positive, bounded, and globally asymptotically stable around the basal values of the equilibrium point [6].

The fundamental idea of such tests is to examine the response of insulin, called insulin sensitivity, after a large amount of glucose is infused into ones body. To this end, several glucose tolerance tests have been developed and applied in clinics and experiments [1, 29–32]. A commonly used protocol is the intravenous glucose tolerance test

¹*Corresponding Author: E-mail: priyaprithu1205@gmail.com,

^{1,2}Ramanujan Institute for Advanced Study in Mathematics, University of Madras,
Chennai -5 Tamil Nadu, India

(IVGTT). One popular approach of the analysis is as follows: (1) formulate or choose a well-formulated model based on physiology. (2) estimate the parameters of the IVGTT model with experimental data, and then (3) the parameter values are used to obtain physiological information, for example, the insulin sensitivity.

All discrete and distributed delay differential equation models for IVGTT explicitly involve a time delay between the rise in glycemia and the correspondingly stimulated insulin secretion. Observable delay effects are often gradual (distributed) and smooth in most physiological systems, it is thus natural to utilize distributed delay parameters rather than discrete. Some authors proposed the IVGTT glucose insulin model with distributed delays [4, 33]. All IVGTT models in [3–5, 34, 35] follow the same criterion, which yields a value of around 20 min. It is well known that a large delay can destabilize a system [11]. An accurate assessment of the delay can therefore play a critical role in elucidation of the metabolic portrait. We then compare the simulation profiles obtained from all these models with two distributed delays also more general and realistic Michaelis-Menten form $\frac{G(t)}{\alpha G(t)+1}$ for the glucose-insulin system is proposed in this article.

The paper is organized as follows. In Section 2, we discuss the model description for kernel delays. In Section 3, we make connections to extend the various stability theorems for our proposed model. We also use the sensitivity functions to evaluate the sensitivity of the glucose-insulin has been analyzed in Section 4. In section 5, we perform numerical calculations and we end this paper with discussion in Section 6.

2 Dynamical Model for the IVGTT glucose-insulin system

2.1 Single - kernal delay models

This section is devoted to present a family of single kernel distributed-delay differential models for the glucose-insulin homeostasis, [4] (the name of the system parameters are the same adopted in [4] where also their meaning is explained):

$$\begin{aligned} \frac{dG(t)}{dt} &= -b_1G(t) - b_4I(t)G(t) + b_7, \\ \frac{dI(t)}{dt} &= -b_2I(t) + b_6 \int_0^\infty \omega(s)G(t-s)ds, \end{aligned} \tag{1}$$

with initial conditions

$$\begin{aligned} G(t) &\equiv G_b, \forall t \in (-\infty, 0), \quad G(0) = G_b + b_0, \\ I(t) &\equiv I_b, \forall t \in (-\infty, 0), \quad I(0) = I_b + b_3b_0. \end{aligned} \tag{2}$$

The parameter involves in system (1) and (2) are described in Table I.

The weight function $\omega(t)$ is a non negative square integrable function defined on $\mathbb{R}^+ = [0, \infty)$ such that

$$\int_0^\infty \omega(t)dt = 1, \quad \int_0^\infty t\omega(t)dt < +\infty \tag{3}$$

The finite quantity $\Delta_a = \int_0^\infty t\omega(t)dt < +\infty$ has the meaning of an average time delay.

In therefore, we define $G(t)$

constant rate spontaneous glucose decay, the second term models the insulin-dependent glucose disappearance rate, while the third term is necessary in order to have an asymptotic decay to the basal glycemia level and $I(t)$ describes the variation of the insulin plasma concentration as a function of two terms: the first models the insulin catabolism (constant rate insulin decay), the second models the pancreatic insulin secretion as an integral function of the past glycemia. Physiologically, the delay integral kernel of equation (2) from system (1) accounts for the sensitivity of the pancreas to the concentration of blood glucose: the pancreas output insulin at a given instant is proportional to a suitably weighted average of the past blood glucose concentrations. A liver first pass effect is taken into account in the second of equation (2) from system (1), where an instantaneous insulin release at time 0, is assumed, proportional to the equivalent concentration of the glucose bolus b_0 .

The model's free parameters are only five (b_0 through b_4). In fact, assuming the subject is at equilibrium at ($G^* = G_b, I^* = I_b$) for a sufficiently long time ($t \rightarrow \infty$), then

$$\begin{aligned} 0 &= -b_1 G_b - b_4 I_b G_b + b_7, \\ 0 &= -b_2 I_b + b_6 G_b. \end{aligned} \tag{4}$$

together imply $b_7 = b_1 G_b + b_4 I_b G_b$, $b_6 = b_2 \frac{I_b}{G_b}$.

As far as what concern the weighting function $\omega(t)$, in the integral in system (1), its shape characterizes the choice of the model according to the features of individuals to whom it is related. For instance, normal individuals, showing a prompt and appropriate insulin response to hyperglycemic stimuli, will likely have a promptly rising and falling ω curve. In the above said model (1), they discussed to guarantee qualitative properties for the entire (albeit smaller) family, without further specification of the kernel ω , subject only to mild integrability conditions. This approach to the numerical quantification of the homeostasis of the glucose insulin system from the mathematical modeling of the IVGTT has the advantage of explicitly representing the two arms of the whole system together (insulin sensitivity of tissues and pancreatic sensitivity to circulating glucose), allowing the eventual simultaneous fitting of glucose and insulin concentration data.

Table I:

Parameters description for the Dynamical model

Parameters	Units	Biological Description
b_0	mg/dl	Theoretical increase in plasma concentration over basal glucose concentration at time zero after instantaneous administration and redistribution of the I.V. glucose bolus
b_1	min^{-1}	Spontaneous glucose first order disappearance rate constant
b_2	min^{-1}	The apparent first order disappearance rate for insulin
b_3	$pM/(mg/dl)$	The first-phase insulin concentration increase, increase in the concentration of glucose at time zero due to the injected bolus
b_4	$min^{-1}pM^{-1}$	The constant amount of insulin-dependent glucose disappearance rate of plasma insulin concentration
b_6	$min^{-1}pM/$ (mg/dl)	The constant amount of second-phase insulin release rate of average plasma glucose concentration per unit time.
b_7	$(mg/dl)min^{-1}$	The constant increase in plasma glucose concentration due to the constant baseline liver glucose

2.2 Double - kernal delay models

An analytic methodology is introduced in order to recast the distributed-delay nonlinear models into a nonlinear systems without delay, in front of an increase of the state space dimension. The availability of real-time data on the insulin concentration is a prerequisite for the development of an artificial pancreas controlling in real time the blood glucose level with optimum insulin infusions from an in vivo pump [33]. They dealt with the problem of the state reconstruction, by applying the theory of asymptotic state observation for nonlinear model systems, has been explored for distributed-delay kernel models of glucose-insulin homeostasis without Michaelis-Menten form $\frac{G(t)}{\alpha G(t)+1}$. In the present section a double-kernel distributed delay model is investigated, which differs from model (1). The delay kernel is also present, where the first kernel $I(t-s)$ must be considered for a change in insulin concentration to affect plasma glucose production, the second kernel $G(t-s)$ denotes the delay before the pancreas can respond to change in blood glucose. We assume instead that the insulin-dependent net glucose tissue uptake takes the more general and realistic Michaelis-Menten form $\frac{G(t)}{\alpha G(t)+1}$, which has maximum capacity $\frac{b_4}{\alpha}$. The parameter α , in the response function $\frac{G(t)}{\alpha G(t)+1}$ is non-negative. $\frac{1}{\alpha}$ is the half-saturation constant. The reason for this is simply due to the limit of time and the capacity of insulin's ability of digesting glucose. Retaining the same names for the parameters used in Table I, the

model is as follows:

$$\begin{aligned} \frac{dG(t)}{dt} &= -b_1G(t) - \frac{b_4G(t)}{\alpha G(t) + 1} \int_0^\infty \omega_I(s)I(t-s)ds + b_7, \\ \frac{dI(t)}{dt} &= -b_2I(t) + b_6 \int_0^\infty \omega_G(s)G(t-s)ds. \end{aligned} \tag{5}$$

with initial conditions

$$\begin{aligned} G(t) &\equiv G_b, \forall t \in (-\infty, 0), \quad G(0) = G_b + b_0, \\ I(t) &\equiv I_b, \forall t \in (-\infty, 0), \quad I(0) = I_b + b_3b_0. \end{aligned} \tag{6}$$

Note that a subscript has been added to the weighting functions ω to distinguish between glucose and insulin kinetics. The properties of the two kernels ω_I and ω_G are similar; in particular conditions (3), are both true. In this work the assumption that $\omega_G(t) \equiv \omega_I(t) \equiv \omega(t)$ as considered, that means $\gamma_I = \gamma_G = \gamma$, according to our model (5). By introducing the following further state components as follows:

$$\begin{aligned} \eta_G(t) &= \int_0^\infty \omega(s)I(t-s)ds, \\ \xi_G(t) &= \int_0^\infty e^{-\gamma(t-s)}I(s)ds, \\ \eta_I(t) &= \int_0^\infty \omega(s)G(t-s)ds, \\ \xi_I(t) &= \int_0^\infty e^{-\gamma(t-s)}G(s)ds. \end{aligned} \tag{7}$$

In order to solve the state estimation problem, a first order differential system has to be achieved from (5). The following nonlinear system is obtained from (5),

$$\begin{aligned} \dot{x}_1(t) &= -b_1x_1(t) - \frac{b_4x_1(t)x_3(t)}{\alpha x_1(t) + 1} + b_7, \\ \dot{x}_2(t) &= -b_2x_2(t) + b_6x_5(t), \\ \dot{x}_3(t) &= -\gamma x_3(t) + \gamma^2 x_4(t), \\ \dot{x}_4(t) &= -\gamma x_4(t) + x_2(t), \\ \dot{x}_5(t) &= -\gamma x_5(t) + \gamma^2 x_6(t), \\ \dot{x}_6(t) &= -\gamma x_6(t) + x_1(t), \end{aligned} \tag{8}$$

where it has been posed:

$$X(t) = \begin{bmatrix} x_1(t) \\ x_2(t) \\ x_3(t) \\ x_4(t) \\ x_5(t) \\ x_6(t) \end{bmatrix} = \begin{bmatrix} G(t) \\ I(t) \\ \eta_G(t) \\ \xi_G(t) \\ \eta_I(t) \\ \xi_I(t) \end{bmatrix} \in \mathbb{R}^6$$

The initial conditions are given below:

$$\begin{aligned} x_1(0) &= G_b + b_0, & x_2(0) &= I_b + b_3b_0, \\ x_3(0) &= I_b, & x_4(0) &= \frac{I_b}{\gamma}, \\ x_5(0) &= G_b, & x_6(0) &= \frac{G_b}{\gamma}. \end{aligned}$$

2.3 Analysis of the model

In this section we study the well-posedness of the model, feasibility region and Lyapunov stability of the unique positive equilibrium for the model (5).

Well-posedness of the model and feasibility region:

In Ref [36], we consider, for each $\alpha > 0$, the Banach space of fading memory type,

$$UC_\alpha = \left\{ \phi \in C((-\infty, 0], \mathbb{R}) : s \rightarrow \phi(s)e^{\alpha s} \text{ is uniformly continuous on } (-\infty, 0] \text{ and } \sup_{s \leq 0} |\phi(s)|e^{\alpha s} < \infty \right\}$$

endowed with the norm

$$\|\phi\|_\alpha = \sup_{s \leq 0} |\phi(s)|e^{\alpha s}. \tag{9}$$

From [37] standard existence and uniqueness results hold for system (5) in UC_α . Next, we analyze (5), in a biologically feasible region for glucose-insulin system.

Proposition 2.1. *As in [38], the time derivatives of the positive solutions (5) are bounded.*

3 Constructions of Stability Analysis

It can be shown that the system admits only one equilibrium point with positive concentrations and the linearized system around the unique equilibrium $(x_1^*, x_2^*, x_3^*, x_4^*, x_5^*, x_6^*)$ by substituting, $u_1 = x_1 - x_1^*, u_2 = x_2 - x_2^*, u_3 = x_3 - x_3^*, u_4 = x_4 - x_4^*, u_5 = x_5 - x_5^*, u_6 = x_6 - x_6^*$ in (8), the model takes the following form,

$$\begin{aligned} \frac{du_1}{dt} &= -\left(b_1 + \frac{b_4x_3^*}{(\alpha x_1^* + 1)^2}\right)u_1 - \frac{b_4x_1^*}{(\alpha x_1^* + 1)}u_3, \\ \frac{du_2}{dt} &= -b_2u_2 + b_6u_5, \\ \frac{du_3}{dt} &= -\gamma u_3 + \gamma^2 u_4, \\ \frac{du_4}{dt} &= -\gamma u_4 + u_2, \\ \frac{du_5}{dt} &= -\gamma u_5 + \gamma^2 u_6, \\ \frac{du_6}{dt} &= -\gamma u_6 + u_1. \end{aligned} \tag{10}$$

The above system (10) takes the matrix form as follows:

$$\dot{x} = Ax \tag{11}$$

where $x = (u_1, u_2, u_3, u_4, u_5, u_6)^T$ and

Proof. let

$$\begin{aligned}
 h_\epsilon(\lambda) &= f_n(\lambda + \epsilon) \\
 &= a_0 + a_1(\lambda + \epsilon) + a_2(\lambda + \epsilon)^2 + a_3(\lambda + \epsilon)^3 + a_4(\lambda + \epsilon)^4 + a_5(\lambda + \epsilon)^5 + a_6(\lambda + \epsilon)^6 \\
 &= \lambda^6 + (6\epsilon + .894)\lambda^5 + (4.470\epsilon + .317 + 15\epsilon^2)\lambda^4 + (1.268\epsilon + 8.940\epsilon^2 + 0.564e^{-1} + 20\epsilon^3)\lambda^3 \\
 &\quad + (1.902\epsilon^2 + .1692\epsilon + 8.940\epsilon^3 + 0.51e^{-2} + 15\epsilon^4)\lambda^2 + (0.2e^{-2} + 6.\epsilon^5 + .1692\epsilon^2 \\
 &\quad + 1.268\epsilon^3 + 4.470\epsilon^4 + 0.102e^{-1}\epsilon)\lambda + 0.355e^{-5} + 0.51e^{-2}\epsilon^2 + 0.2e^{-2}\epsilon \\
 &\quad + 0.564e^{-1}\epsilon^3 + .894\epsilon^5 + \epsilon^6 + .317\epsilon^4
 \end{aligned}$$

$$M_{h_\epsilon} = \begin{bmatrix} 0.102e^{-1}\epsilon + 0.2e^{-2} & 0.2e^{-2}\epsilon + 0.355e^{-5} & 0 & 0 & 0 & 0 \\ 8.940\epsilon^2 + 1.268\epsilon & .1692\epsilon + 0.51e^{-2} & 0.102e^{-1}\epsilon + 0.2e^{-2} & 0.2e^{-2}\epsilon + 0.355e^{-5} & 0 & 0 \\ 6\epsilon + .894 & 4.470\epsilon + .317 & 8.940\epsilon^2 + 1.268\epsilon & .1692\epsilon + 0.51e^{-2} & 0.102e^{-1}\epsilon + 0.2e^{-2} & 0.2e^{-2}\epsilon + 0.355e^{-5} \\ 0 & 0 & 6\epsilon + .894 & 4.470\epsilon + .317 & 8.940\epsilon^2 + 1.268\epsilon & .1692\epsilon + 0.51e^{-2} \\ 0 & 0 & 0 & 1 & 6\epsilon + .894 & 4.470\epsilon + .317 \\ 0 & 0 & 0 & 0 & 0 & 1 \end{bmatrix},$$

and

$$M_{G_\epsilon} = \begin{bmatrix} 0.102e^{-1}\epsilon + 0.2e^{-2} & 0.2e^{-2}\epsilon + 0.355e^{-5} & 0 & 0 & 0 & 0 \\ 1.268\epsilon & .1692\epsilon + 0.51e^{-2} & 0.102e^{-1}\epsilon + 0.2e^{-2} & 0.2e^{-2}\epsilon + 0.355e^{-5} & 0 & 0 \\ 6\epsilon + .894 & 4.470\epsilon + .317 & 1.268\epsilon & .1692\epsilon + 0.51e^{-2} & 0.102e^{-1}\epsilon + 0.2e^{-2} & 0.2e^{-2}\epsilon + 0.355e^{-5} \\ 0 & 0 & 6\epsilon + .894 & 4.470\epsilon + .317 & 1.268\epsilon & .1692\epsilon + 0.51e^{-2} \\ 0 & 0 & 0 & 1 & 6\epsilon + .894 & 4.470\epsilon + .317 \\ 0 & 0 & 0 & 0 & 0 & 1 \end{bmatrix}.$$

Now we compute the major subdeterminants of M_{G_ϵ} as follows:

$$\begin{aligned}
 \Delta_1 &= 0.102e^{-1}\epsilon + 0.2e^{-2} > 0, \\
 \Delta_2 &= \begin{bmatrix} 0.102e^{-1}\epsilon + 0.2e^{-2} & 0.2e^{-2}\epsilon + 0.355e^{-5} \\ 1.268\epsilon & .1692\epsilon + 0.51e^{-2} \end{bmatrix} > 0, \quad \text{when } 0 < \epsilon \ll 1.
 \end{aligned}$$

Proceeding like this way, we get

$$\Delta_6 > 0, \quad \text{when } 0 < \epsilon \ll 1.$$

Hence

$$h_\epsilon(\lambda) = f_n(\lambda + \epsilon)$$

□

Now, we consider the general n -dimensional autonomous system:

$$\frac{dx}{dt} = f(x), \quad f(0) = 0, \tag{12}$$

where $x = (x_1, \dots, x_n)^T \in \mathbb{R}^n, f = (f_1, f_2, \dots, f_n) \in C[\Omega_h, \mathbb{R}]$, where $\Omega_h = \{x : \|x\| \leq h\}$.

Theorem 3.3. *let the zero solution of (11) and $V(x) : \mathbb{R}^6 \rightarrow \mathbb{R}$ be a continuous differentiable function (denoted by, $V(x) \in C^1[\mathbb{R}^6, \mathbb{R}]$) such that*

- (i) $V(0) = 0$,
- (ii) $V(x) > 0 \in \mathbb{R}^6 - \{0\}$,
- (iii) $\dot{V}(x) \leq 0 \in \mathbb{R}^6 - \{0\}$.

when $x \geq 1$, then the zero solution is stable.

Theorem 3.4. *If there exists positive definite function $V(x) \in C^1[\mathbb{R}^6, \mathbb{R}]$ such that*

$$\frac{dV}{dt} < 0,$$

then the set $S = \{x | \frac{dV}{dt} = 0, x \in \mathbb{R}^6\}$ excludes $x = 0$, i.e., it does not include all positive half trajectories which are nonzero. Then, the zero solution of (11) is said to be asymptotically stable, if $x = 1$

Proof. Choose a Lyapunov function,

$$V(x) = xe^{-x}, \tag{13}$$

When $0 < xe^{-x} < x$, V is positive definite, and

$$\begin{aligned} \frac{dV}{dt} &= \frac{\partial V}{\partial x} \frac{dx}{dt}, \\ &= -e^{-x}(x-1)Ax \quad \text{if } x = 1, \\ &\leq 0. \end{aligned}$$

Let $\frac{dV}{dt} = 0$ yields $S = \{x | x = 0\}$. But $x = 0$, does not include all positive half trajectories which are nonzero. Therefore, the zero solution of (11) is asymptotically stable \square

Definition 3.2. [39] *If a function $\phi \in [\mathbb{R}^+, \mathbb{R}^+]$, where $\mathbb{R}^+ = [0, +\infty)$, or $\phi \in C([0, h], \mathbb{R}^+)$ is monotonically strictly increasing, and $\phi(0) = 0$, we call ϕ a Wedge function, or simply call it a K class function, denoted by $\phi \in K$.*

Definition 3.3. [39] *Let the zero solution of (12) is said to be uniformly stable with respect to t_0 , if $\forall \epsilon > 0, \exists \delta(\epsilon) > 0$ ($\delta(\epsilon)$ is independent of t_0) such that $\|x_0\| < \delta$, implies $\|x(t, t_0, x_0)\| < \epsilon$ for $t \geq t_0$.*

Theorem 3.5. *The zero solution of (11), is uniformly stable if and only if $V(x) \in C^1[\mathbb{R}^6, \mathbb{R}]$ with infinitesimal bound such that*

$$D^+V(x) \leq 0.$$

Proof. Using the given condition, $\exists \phi_1, \phi_2 \in K$ such that

$$\phi_1(\|x\|) \leq V(x) \leq \phi_2(\|x\|),$$

Then, $\forall \epsilon > 0 (\epsilon < h)$ such that by taking $\delta = \phi_2^{-1}(\phi_1(\epsilon))$, i.e., $\epsilon = \phi_1^{-1}(\phi_2(\delta))$, here the initial condition $t_0 = 0$, then we have,

$$\phi_1(\|x(t, 0, x_0)\|) \leq V(x(t, 0, x_0)) \leq V(x_0) \leq \phi_2(\|x_0\|) < \phi_2(\delta), \tag{14}$$

when $\|x_0\| < \delta$, it follows that

$$\|x(t, 0, x_0)\| \leq \phi_1^{-1}(\phi_2(\delta)) = \epsilon, \text{ for } t \geq 0.$$

However, $\delta = \phi_2^{-1}(\phi_1(\epsilon)) = \delta(\epsilon)$ is independent of (t_0) , here $t_0 = 0$. So, the zero solution of (11) is uniformly stable.

To prove the necessary condition, let we construct

$$V(x) = xe^{-x} \inf_{0 \leq \tau \leq t} \|\eta(\tau, t, x)\|$$

then $V(x)$ is continuous, and $V(x) \leq x\|\eta(\tau, t, x)\| = x\|x\|$. So $V(x)$ is infinitesimally upper bounded.

Next we prove that $V(x)$ is positive definite. Since the zero solution of (11) is uniformly stable, $\forall \epsilon > 0, \exists \delta(\epsilon)$, when $\|q\| < \delta$, for all $\tau \geq 0$ and $t \geq \tau$, we have

$$\|x(\tau, t, q)\| < \epsilon, \tag{15}$$

when $\epsilon < \|x\| \leq h$, for all $t \geq \tau \geq 0$, we have,

$$\eta(\tau, t, x) \geq \delta > 0.$$

Otherwise, for certain $\tau^*, x^*, t^*, \epsilon \leq \|x^*\| \leq h, 0 \leq \tau^* \leq t^*$. We obtain,

$$\|\eta(\tau^*, t^*, x^*)\| > \delta.$$

If we take $q = \eta(\tau^*, t^*, x^*)$, then we get $x^* = \|\eta(t^*, \tau^*, q)\|$. Using the Definition 3.2, when $\|q\| = \|\eta(\tau^*, t^*, x^*)\| < \delta, \eta(t^*, \tau^*, q) < \epsilon$ holds for all $t = t^* \geq \tau^*$. which contradicts that $\|x^*\| \geq \epsilon$. Therefore (15) is true. Hence $V(x)$ is positive definite.

And now we have to prove that $D^+V(x) \leq 0$. Since $x = \eta(t, 0, q)$ along an arbitrary solution of (11), we have,

$$\begin{aligned} V(x) &= V(\eta(t, 0, q)), \\ &= xe^{-x} \inf_{0 \leq \tau \leq t} \|\eta(\tau, t, (\eta(t, 0, q)))\|, \\ &= xe^{-x} \inf_{0 \leq \tau \leq t} \|\eta(\tau, 0, q)\|. \end{aligned}$$

To see that $V(x)$ is a monotone function of x . As a result, $D^+V(x) \leq 0$ is true. Hence the proof. □

Definition 3.4. [39] In general for autonomous system, the function $W(x) \in C[\mathbb{R}^n, \mathbb{R}]$ is said to be positive definite and radially unbounded if $W(x)$ is positive definite and $x \rightarrow \infty$ implies $W(x) \rightarrow \infty$.

Remark 3.

- (i) The above above Definition 3.4 does not hold for our system (11).
- (ii) Therefore the radially unbounded condition does not hold for our positive definite function.
- (iii) Hence our system (11) is not globally asymptotically stable.

Theorem 3.6. Let $f(x) \in C^1[\mathbb{R}^6, \mathbb{R}]$, $f(0) = 0$, and f satisfy the Lipschitz condition for x . Then the zero solution of (11), is globally exponentially stable if and only if there exists $V(x) \in C^1[\mathbb{R}^6, \mathbb{R}]$, such that

- (i) $\|x\| \leq V(x) \leq K(\alpha)\|x\|$, $x \in S_\alpha = \{x : \|x\| \leq \alpha, \alpha > 0\}$;
- (ii) $\frac{dV(x)}{dt} \leq -pqV(x)$, where $0 < p < 1, q > 0, p, q$ are constants.

Proof. For all $\alpha > 0$ when $x_0 \in S_\alpha$, let $x(t) = x(t, 0, x_0)$ be the solution of (11) and $t_0 = 0$, by condition (ii), we have

$$\frac{dV(x)}{dt} \leq -pqV(x).$$

Now, we consider the comparison equation,

$$\frac{du}{dt} = -pqu.$$

Let $u_0 = V(x_0)$, then

$$u(t, 0, u_0) = u_0e^{-pqt},$$

We obtain

$$V(x) \leq u_0e^{-pqt} = V(x_0)e^{-pqt}, \quad t \geq 0.$$

By conditions (i), we have

$$\|x\| \leq V(x) \leq K(\alpha)\|x_0\|e^{-pqt} \leq K(\alpha)\|x_0\|e^{-\lambda t}, \quad \lambda = pq, \tag{16}$$

i.e.,

$$\|x(t, 0, x_0)\| \leq K(\alpha)\|x_0\|e^{-\lambda t}, \quad t \geq 0.$$

So the zero solution of (11) is globally exponentially stable.

To prove the necessary condition, let the zero solution of (11) be globally exponentially stable. Then there exists constant $q > 0$ such that $\forall \alpha > 0, \exists K(\alpha) > 0$, when $x_0 \in S_\alpha$,

$$\|x(t, 0, x_0)\| \leq K(\alpha)\|x_0\|e^{-pt} \text{ holds.}$$

For $0 < q < 1$, define a function:

$$V(x) = \sup_{\tau \geq 0} \|x(t + \tau, x)\| e^{pq\tau}.$$

Then, $\forall x \in S_\alpha$, we have

(i)

$$\begin{aligned} \|x\| \leq V(x) &\leq \sup_{\tau \geq 0} K(\alpha) \|x\| e^{-p\tau} e^{pq\tau}, \\ &\leq K(\alpha) \|x\| \sup_{\tau \geq 0} e^{-(1-q)p\tau}, \\ &\leq K(\alpha) \|x\|. \end{aligned}$$

i.e.,

$$\|x\| \leq V(x) \leq K(\alpha) \|x\|.$$

(ii) let $x^* = x(t + h, x)$. It follows that,

$$\begin{aligned} V(x + h, x^*) &= \sup_{\tau \geq 0} \|x(t + h + \tau, x^*)\| e^{pq\tau}, \\ &= \sup_{\tau \geq 0} \|x(t + h + \tau, x)\| e^{pq\tau}, \\ &\leq \sup_{\tau \geq 0} \|x(t + h, x)\| e^{pq\tau} e^{-(pqh)}, \\ &= V(x) e^{-(pqh)}. \end{aligned}$$

Furthermore, we obtain

$$\frac{V(x + h, x^*) - V(x)}{h} = V(x) \frac{e^{-(pqh)} - 1}{h}.$$

Now, we have

$$\begin{aligned} \frac{dV(x)}{dt} &= \lim_{h \rightarrow 0} \frac{V(x + h, x^*) - V(x)}{h}, \\ &\leq \lim_{h \rightarrow 0} V(x) \frac{e^{-(pqh)} - 1}{h}, \\ &= V(x) \lim_{h \rightarrow 0} \frac{e^{-(pqh)} - 1}{h}, \\ &= -pqV(x). \end{aligned}$$

i.e.,

$$\frac{dV(x)}{dt} \leq -pqV(x).$$

Hence the proof. □

Remark 4. *Summing up, we conclude that the zero solution x of (11) is said to be stable, asymptotically stable, uniformly stable and globally exponentially stable, if $x \geq 1$.*

4 Sensitivity Analysis

The possibility to reliably estimate an index of sensitivity is essential to any model which aims at being useful to diabetologists. Parameters in the dynamical system exerting the most influence on the system state can be established through sensitivity analysis. Here, we show the sensitivity analysis with respect to the parameter is considered. It is quite usual for a model to display high sensitivity to small variations in some parameters, while displaying robustness to variations in other parameters. However, for simplicity we will use the so called “direct approach” to find sensitivity functions of system (10) in [40]. In the following the sensitivity functions with respect to an arbitrary parameter q , for the system (10), are denoted by,

$$u_{i,q} = \frac{\partial u_i(t)}{\partial q}, \quad i = 1, 2, \dots, n \tag{17}$$

The corresponding sensitivity system (10) with respect to the parameter ‘ b_6 ’ is as follows,

$$\begin{aligned} u_{1,b_6} &= -\left(b_1 + \frac{b_4 u_3}{(\alpha u_1^* + 1)^2}\right) u_{1,b_6}(t, b_6) - \frac{b_4 u_1^*}{(\alpha u_1^* + 1)} u_{3,b_6}(t, b_6), \\ u_{2,b_6} &= -b_2 u_{2,b_6}(t, b_6) + b_6 u_{5,b_6}(t, b_6) + u_5(t), \\ u_{3,b_6} &= -\gamma u_{3,b_6}(t, b_6) + \gamma^2 u_{4,b_6}(t, b_6), \\ u_{4,b_6} &= -\gamma u_{4,b_6}(t, b_6) + u_{2,b_6}(t, b_6), \\ u_{5,b_6} &= -\gamma u_{5,b_6}(t, b_6) + \gamma^2 u_{6,b_6}(t, b_6), \\ u_{6,b_6} &= -\gamma u_{6,b_6}(t, b_6) + u_{1,b_6}(t, b_6). \end{aligned} \tag{18}$$

The corresponding sensitivity system (10) with respect to the parameter ‘ b_4 ’ is as follows,

$$\begin{aligned} u_{1,b_4} &= -\left(b_1 + \frac{b_4 u_3^*}{(\alpha u_1^* + 1)^2}\right) u_1(t) - \frac{b_4 u_1^*}{(\alpha u_1^* + 1)^2} u_{3,b_4}(t, b_4) \\ &\quad - \frac{u_1^*}{(\alpha u_1^* + 1)} u_3(t) - \frac{u_3^*}{(\alpha u_1^* + 1)^2} u_1(t), \\ u_{2,b_4} &= -b_2 u_{2,b_4}(t, b_4) + b_6 u_{3,b_4}(t, b_4), \\ u_{3,b_4} &= -\gamma u_{3,b_4}(t, b_4) + \gamma^2 u_{4,b_4}(t, b_4), \\ u_{4,b_4} &= -\gamma u_{4,b_4}(t, b_4) + u_{2,b_4}(t, b_4), \\ u_{5,b_4} &= -\gamma u_{5,b_4}(t, b_4) + \gamma^2 u_{6,b_4}(t, b_4), \\ u_{6,b_4} &= -\gamma u_{6,b_4}(t, b_4) + u_{1,b_4}(t, b_4). \end{aligned} \tag{19}$$

The semi-relative sensitivity solutions (depicted in Fig.1(a)-4(f)) are calculated by simply multiplying the unmodified sensitivity solutions by a chosen parameter which provides information concerning the amount the state will change when that parameter is doubled (i.e., a perturbation on the order of b_6 and b_4). It is best to calculate this type of sensitivity solution to obtain a more thorough understanding of the dynamics.

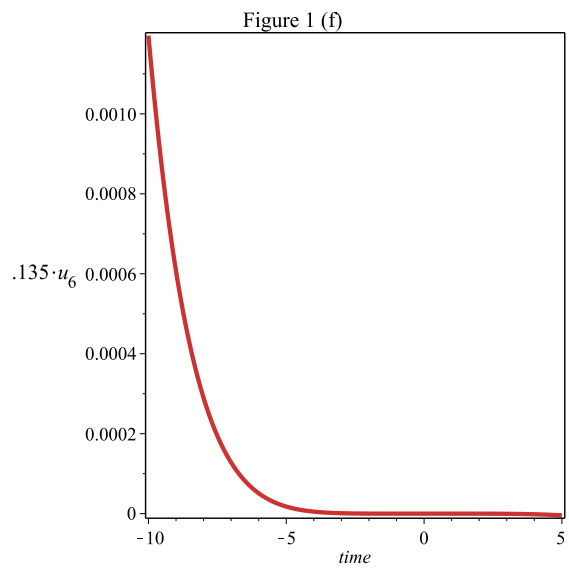
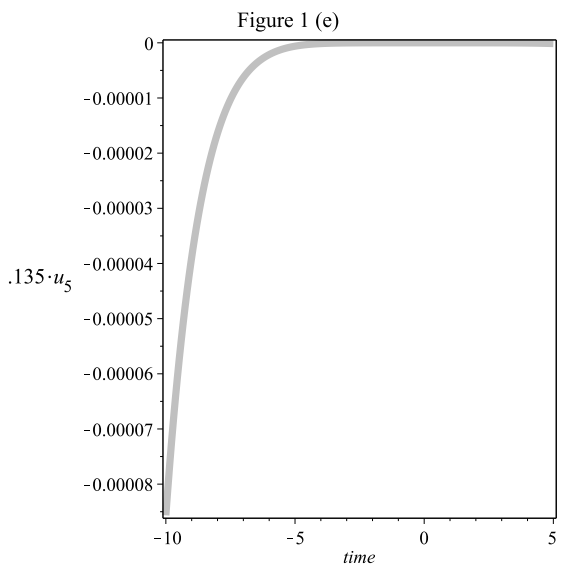
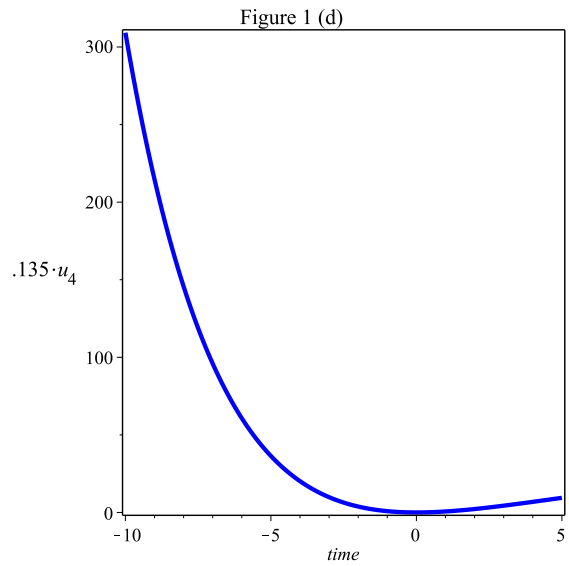
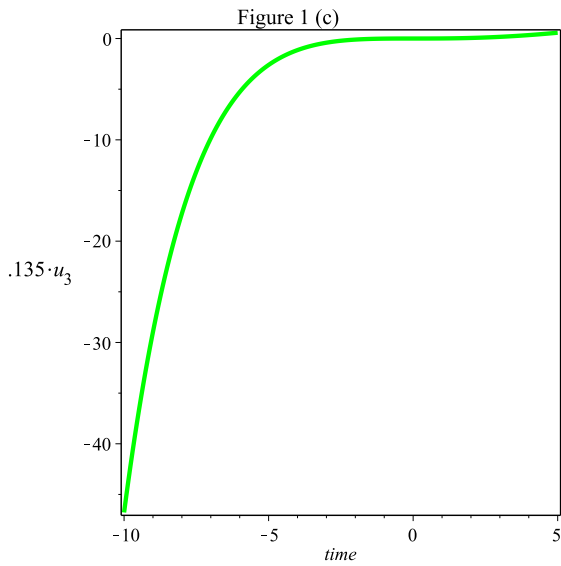
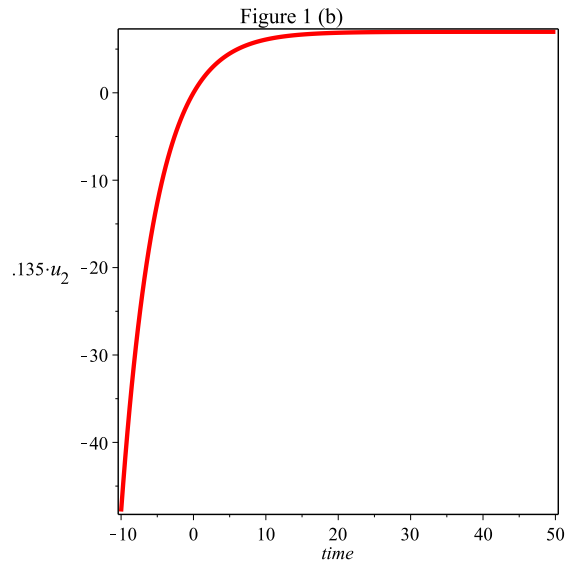
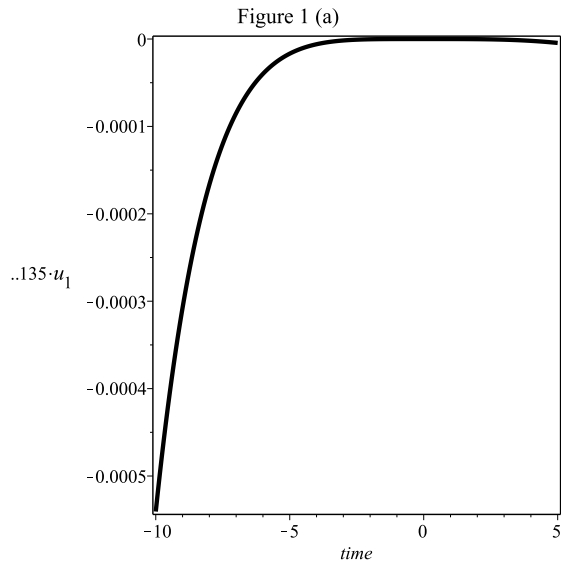
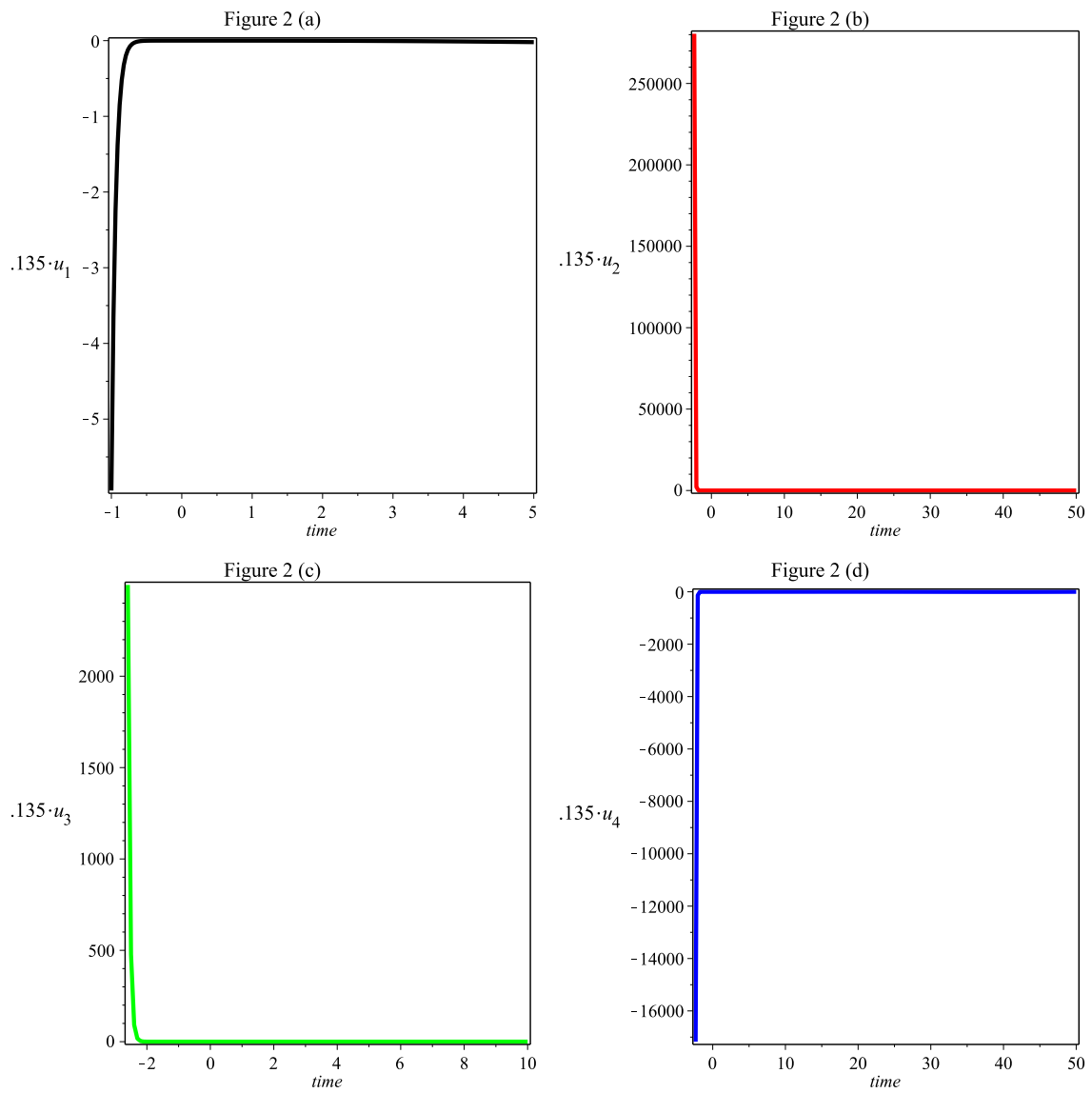


Fig. 1(a)-1(f) show the semi-relative sensitivity analysis for the system (18) is subject to F1 data, from Table II respectively.



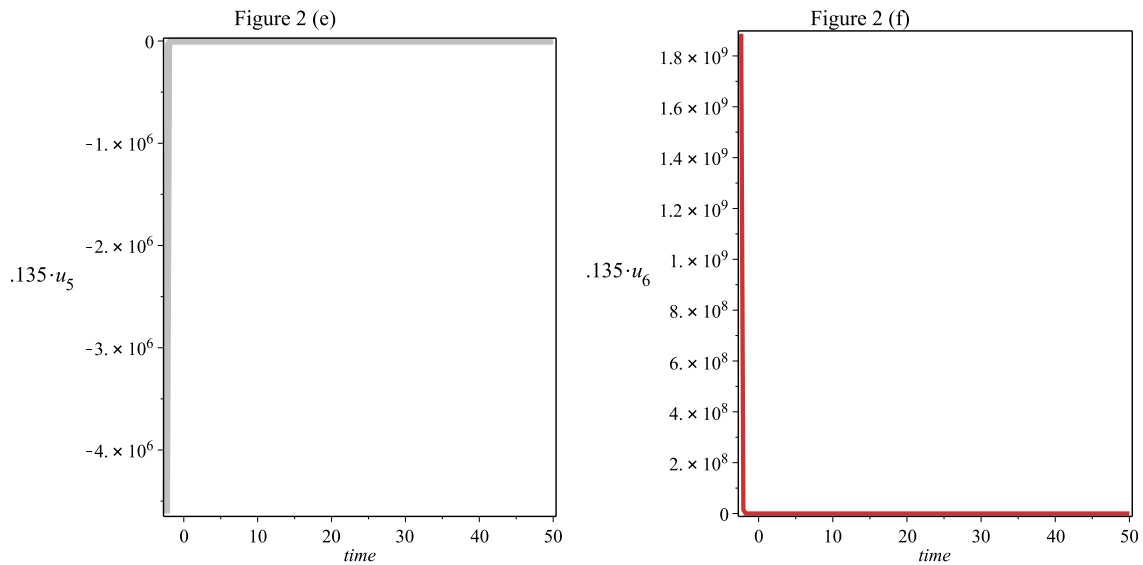
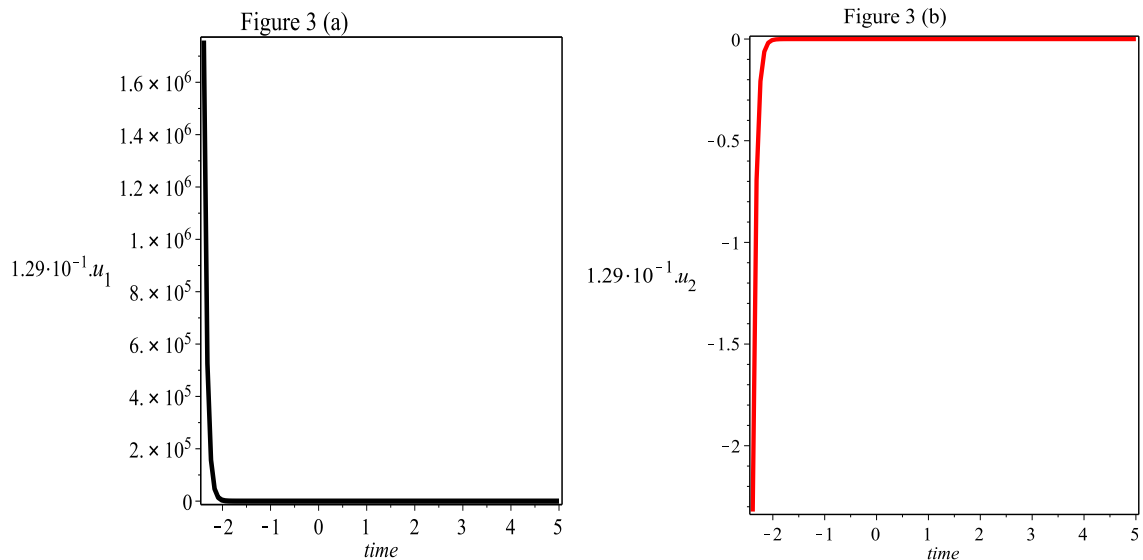


Fig. 2(a)-2(f) show the semi-relative sensitivity analysis for the system (18) is subject to R1 data, from Table II respectively.

Comparison between the plots 1(a) - 2(f) show that, the parameter b_6 is sensitive in 1(d), 1(f), 2(b), 2(c) and 2(f). Therefore we observe that small change in b_6 (*i.e.*, The constant amount of second-phase insulin release rate of average plasma glucose concentration per unit time) can produce significant changes in the above said figures. Other than the remaining figures show that negatively proportion with increasing the initial function and it is very sensitive in the early time intervals and the sensitivity decreases by time to be insensitive in the steady state.



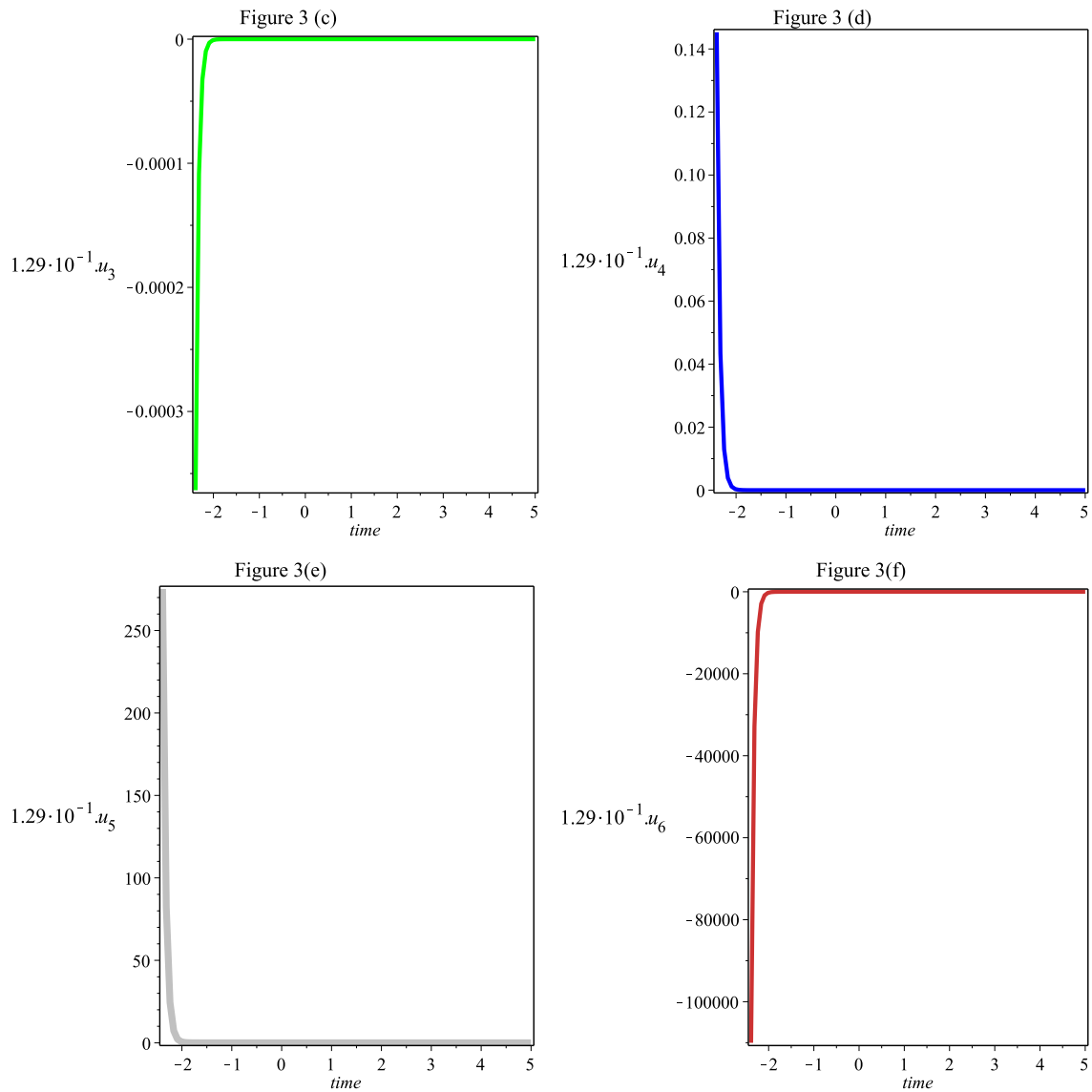


Fig. 3(a)- 3(f) show the semi-relative sensitivity analysis for the system (19), is subject to F1 data, from Table II respectively.

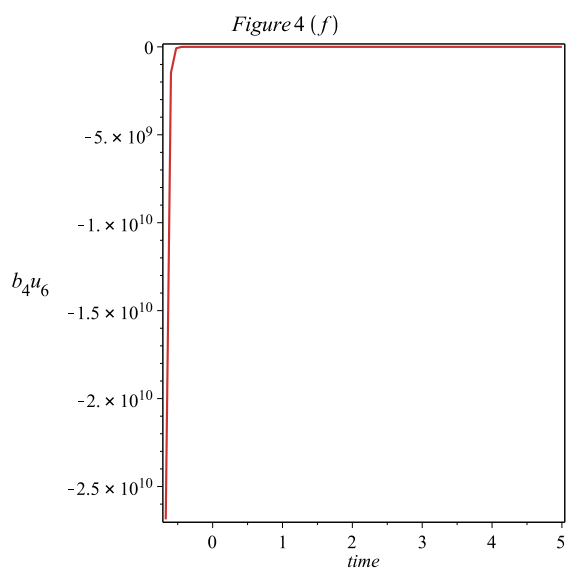
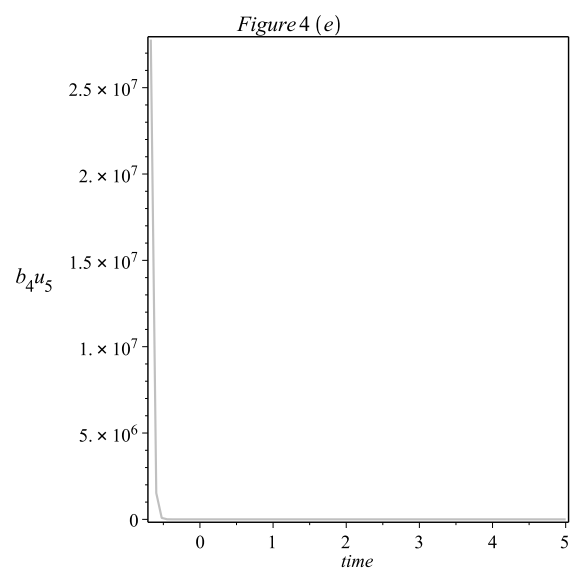
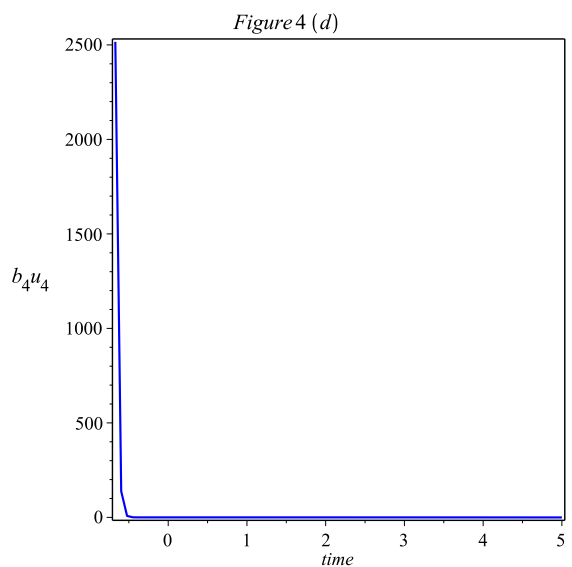
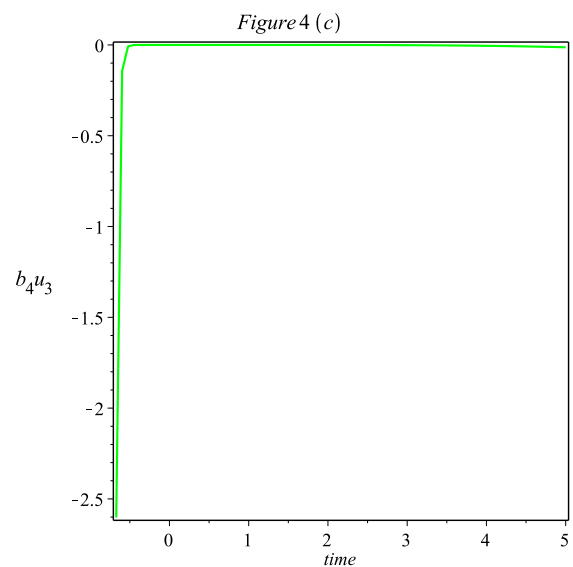
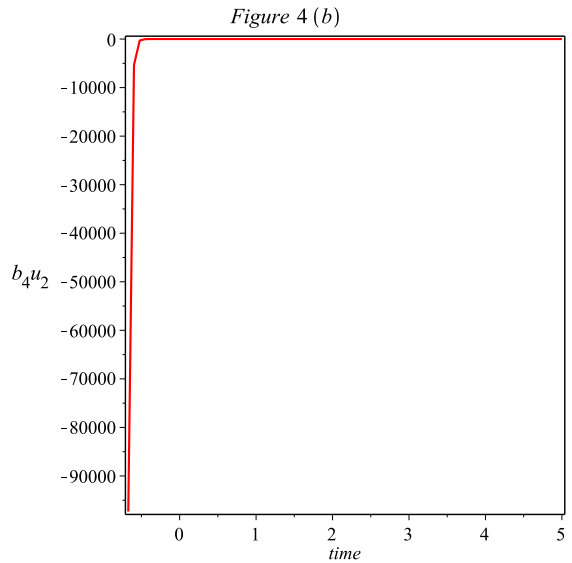
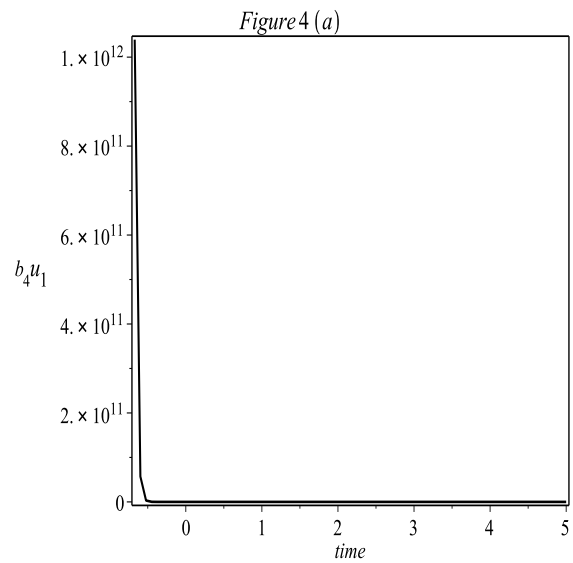


Fig. 4(a)-4(f) show the semi-relative sensitivity analysis for the system (19) subject to R1 data, from Table II respectively.

Comparison between the plots 3(a) - 4(f) show that, the parameter b_4 is sensitive in 3(a), 3(d), 3(e), 4(a), 4(d) and 4(e). Therefore we observe that small change in b_4 (*i.e.*, The constant amount of insulin-dependent glucose disappearance rate of plasma insulin concentration) can produce significant changes in the above said figures. Other than the remaining figures show that negatively proportion with increasing the initial function and it is very sensitive in the early time intervals and the sensitivity decreases by time to be insensitive in the steady state.

5 Application and Numerical Illustration

In this section, we carry out some numerical illustrations to display the qualitative behaviours of model (10) (see Figs. 6 (a)-10), fit the model to experimental data of glucose insulin homeostasis. We present the graphical representation of the dynamical system with a set of parameter values in Table II, using with the commercial software package as MAPLE.

Data from 40 healthy volunteers (18 males and 22 females, average anthropometric characteristics reported in Table II), who had been previously studied in several protocols at the Catholic University Department of Metabolic Diseases were analyzed in [35]. All subjects had negative family and personal histories for Diabetes Mellitus and other endocrine diseases, were on no medications, had no current illness and had maintained a constant body weight for the six months preceding each study. For the three days preceding the study each subject followed a standard composition diet (55% carbohydrate, 30% fat, 15% protein) ad libitum with at least 250 g carbohydrates per day.

We also compare the solution (10), using the Table II data values for our model. It is known that unique equilibrium point is stable if all the roots of the characteristic equations of (10) have negative real parts. (roots are located on the open left side of the complex plane *i.e.*, $Re \lambda_i < 0, i = 1, 2, \dots, 6$).

The following Table III contains the eigenvalue for the unique positive steady states. The values γ is taken from [33] and other parameter values are taken from [38]. Here R1 and R2 denote the minimum and maximum range values for 40 subjects healthy volunteers and these values are taken from [35].

Table II: Parameter values for the Dynamical model

Subject	$x_1(0)$	$x_2(0)$	$x_3(0)$	$x_4(0)$	$x_5(0)$	$x_6(0)$	b_1	b_2	b_4	b_6	b_7	Source
F1	320	907.25	51.7	258.5	79	395	0.0509	0.2062	$1.29E-07$	0.135	4.02	[6]
R1	17.445	18.920088	18.92	94.6	4.03	20.15	0.016	0.061	0.425	0.136	618.82	[35]
R2	18.465	62.68008840	62.68	313.4	5.05	25.25	0.016	0.061	0.425	0.136	618.82	[35]

Table III: The computed eigenvalues of the characteristic equation of (10) at the unique steady state, corresponding to the value of $\alpha = 0.01$ and $\gamma = 0.2$ are presented here. The other parameter values are taken from Table II.

Subject	Eigenvalues for the unique steady state $(x_1^*, x_2^*, x_3^*, x_4^*, x_5^*, x_6^*)$
F1	$-0.2102480670 + 0.2485809627 \times 10^{-1}I, -0.1791492656 + 0.1682367033 \times 10^{-1}I,$ $-0.5087274240 \times 10^{-1}I, -0.2274329705, -0.1791492656 - 0.1682367033 \times 10^{-1}I,$ $-0.2102480670 - 0.2485809627 \times 10^{-1}I$
R1	$-0.2703676998 \times 10^{-1}, -0.1126413675 + 0.1704186557I,$ $-0.3313769006 + 0.1093735322I, -0.5845630317,$ $-0.3313769006 - 0.1093735322I, -0.1126413675 - 0.1704186557I$
R2	$-0.1263652490 + 0.1317770531I, -0.3008003140 + 0.8512086584 \times 10^{-1}I,$ $-0.6668873551 \times 10^{-2}, -0.1899781779,$ $-0.3008003140 - 0.8512086584 \times 10^{-1}I, -0.1263652490 - 0.1317770531I$

5.1 Applications

For example, when

$$b_1 = 0.0509, b_2 = 0.2062, b_4 = 0.000000129, b_6 = 0.135, \gamma = 0.2, \alpha = 0.01, x_1^* = 78.9726, x_3^* = 51.7037,$$

these parameter values are taken from the experimental subject in [6]. The system (5), as follows

$$\begin{aligned} \frac{dG(t)}{dt} &= -0.0509G(t) - \frac{0.000000129G(t)}{0.01G(t) + 1} \int_0^\infty \omega_I(s)I(t-s)ds + 4.02, \\ \frac{dI(t)}{dt} &= -0.2062I(t) + 0.135 \int_0^\infty \omega_G(s)G(t-s)ds. \end{aligned} \tag{20}$$

The unique positive steady state (G^*, I^*) is given by

$$G^* = 78.9726, \quad I^* = 51.7037$$

It is easy to verify that the conditions of Theorem 3.3, for using the initial conditions (Table II), we proceed the linearized system for (20) as follows,

$$\begin{aligned} \frac{dx_1(t)}{dt} &= -\left(0.0509 + \frac{0.000000129 \times 51.7037}{(0.01 \times 78.9726 + 1)^2}\right)x_1(t) - \frac{0.000000129 \times 78.9726}{(0.01 \times 78.9726 + 1)}x_3(t), \\ \frac{dx_2(t)}{dt} &= 0.2062x_2(t) + 0.135x_5(t), \\ \frac{dx_3(t)}{dt} &= -0.2x_3(t) + 0.04x_4(t), \\ \frac{dx_4(t)}{dt} &= -0.2x_4(t) + x_2(t), \\ \frac{dx_5(t)}{dt} &= -0.2x_5(t) + 0.04x_6(t), \\ \frac{dx_6(t)}{dt} &= -0.2x_6(t) + x_1(t). \end{aligned} \tag{21}$$

and the characteristic equation of (21) becomes,

$$\begin{aligned} \Delta(\lambda) &= \lambda^6 + 1.057100378\lambda^5 + .4561759604\lambda^4 + .1021006171\lambda^3 \\ &\quad + 0.1234617001 \times 10^{-4}\lambda^2 + 0.7472216598 \times 10^{-4}\lambda \\ &\quad + 0.1679092976 \times 10^{-4} \end{aligned} \tag{22}$$

We obtain the characteristic roots (22), are as follows,

$$\begin{aligned} &-.2102480670 + 0.2485809627 \times 10^{-1}I, \quad -.1791492656 + 0.1682367033 \times 10^{-1}I, \\ &\quad \quad \quad -.5087274240 \times 10^{-1}, \quad -.2274329705, \\ &-.1791492656 - 0.1682367033 \times 10^{-1}I, \quad -.2102480670 - 0.2485809627 \times 10^{-1}I \end{aligned} \tag{23}$$

Now, we conclude that the IVGTT system (21), take the data for subject F1, all the characteristic roots of the characteristic equation for the Generic IVGTT model have

negative real parts. Therefore the above system (21) is always stable. The plots of the characteristic equations as shown in Fig 5 (a) and 5 (b). Similarly we can prove that for 40 healthy volunteers subjects R1 and R2.

Fig. 5 (a) - 7 (b) shows that the glucose and insulin level for F1, R1 and R2 data for different values of α .

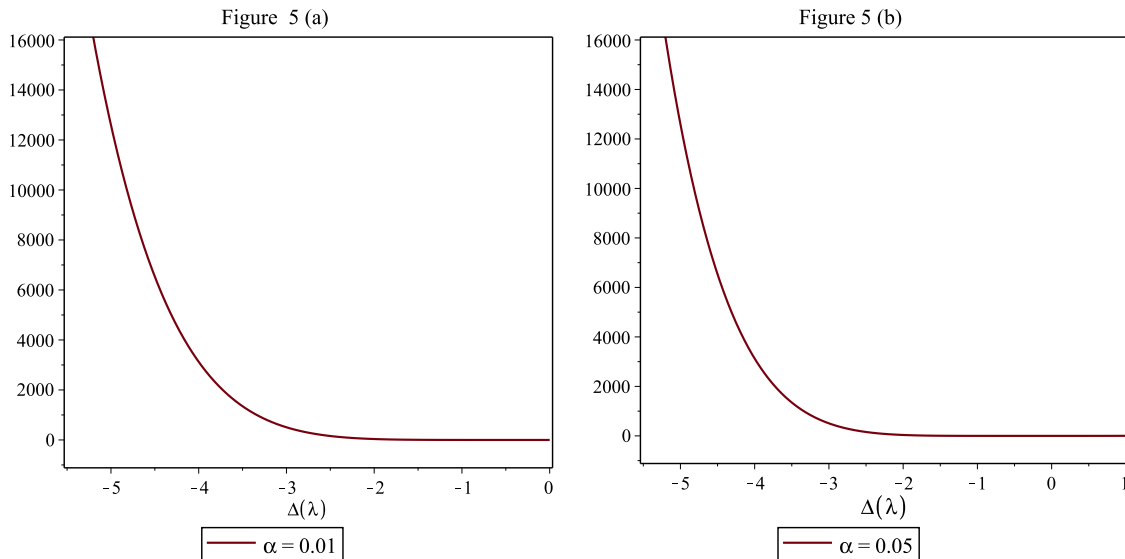


Fig. 5 (a) and 5 (b): Plots the characteristic equation of (22) for the subject data F1 with different values of α .

Fig. 6 (a) - 7 (b) shows the minimum and maximum range value for 40 healthy volunteers of R1 and R2 data. The plots of the characteristic equation of the original system (10), as shown below. The values are taken from Table II.

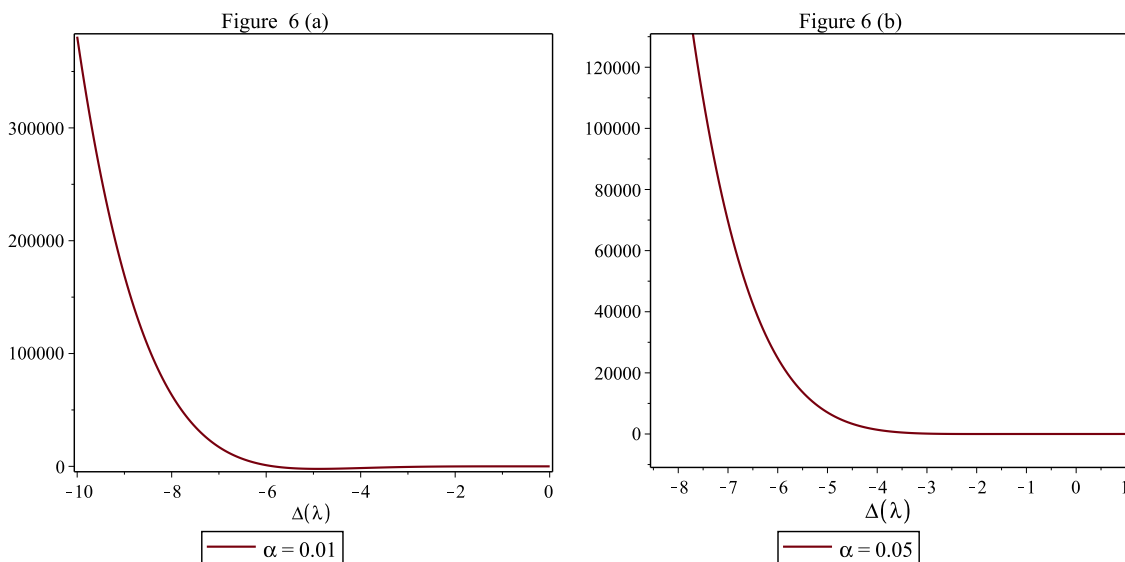


Fig. 6 (a) and 6 (b): Plots the characteristic equation of (10) for the subject data R1 with different values of α .

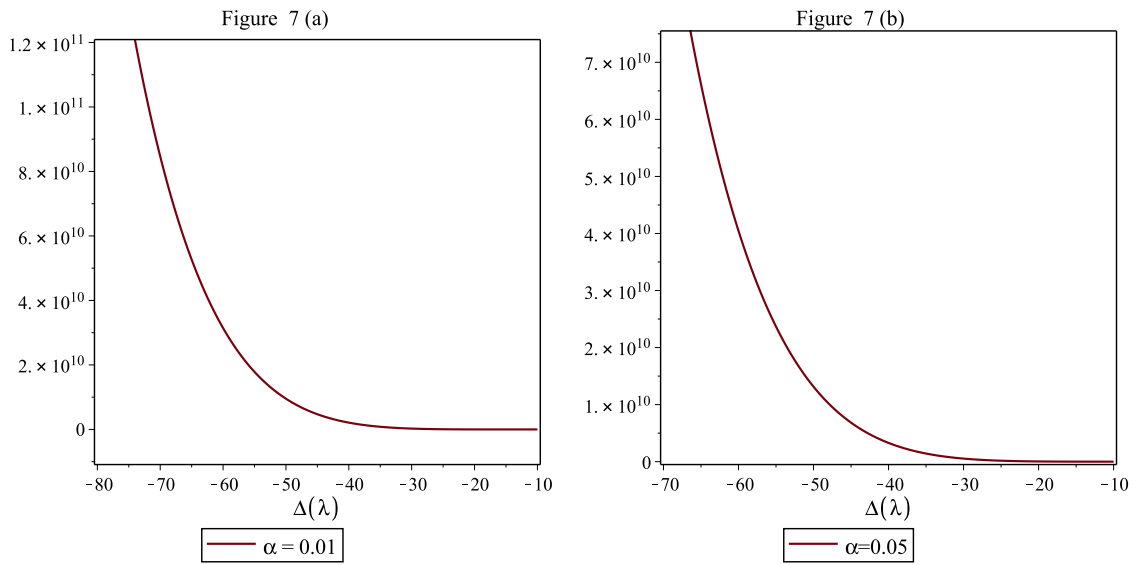


Fig. 7 (a) and 7 (b): Plots the characteristic equation of (10) for the subject data R2 with different values of α .

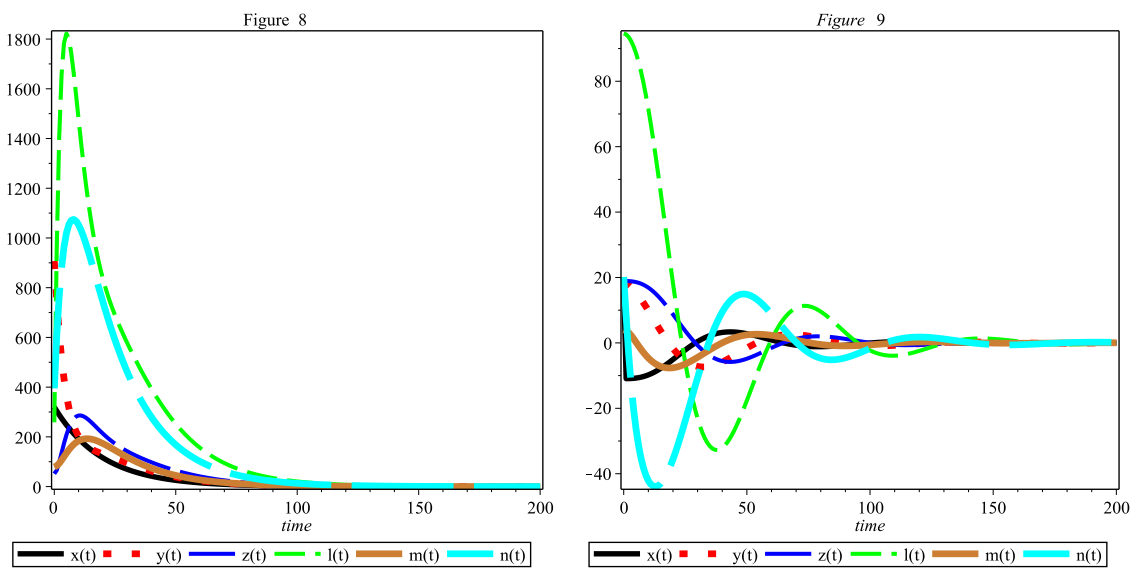


Fig. 8. shows the solution trajectories of the system (21) versus time together with the predicted time curves for the subject data F1.

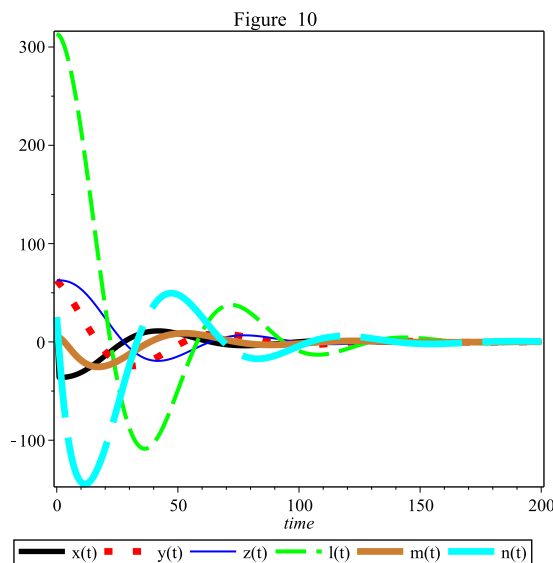


Fig. 9 and 10 show the solution trajectories of the system (10) versus time together with the predicted time curves for the subject data R1 and R2.

Figure 8,9 and 10 portray three typical subjects with both insulin and glucose concentration observations for the model (10). For the Minimal model, fitting was performed by means of a Weighted Least Squares (WLS) estimation procedure, considering as weights the inverse of the squares of the expectations and as coefficient of variation 1.5 percentage for glucose and 7 percentage for insulin [1]. Here, our proposed model dealt for F1 data and also the Anthropometric characteristic of subjects studied for R1 and R2 with Weighted Least Square method. Comparison between all the mentioned data (Table II) attained stable, if all the roots of the corresponding characteristic equation having negative real parts. The plot of the characteristic equation and solution trajectories can be proved by analytically (see Figures. 5(a)-7(b) and 8-10) for the different values of α .

5.2 Adomain decomposition method: Numerical Illustration

Adomian decomposition method is a powerful tool which enables to find analytical solutions in case of our non-linear equations (10). This method has been successfully applied to a system (10). For the non-linear systems, we usually derive a very good approximations to the solutions and it was shown in figure (Using the Table II, we can see for F1 data).

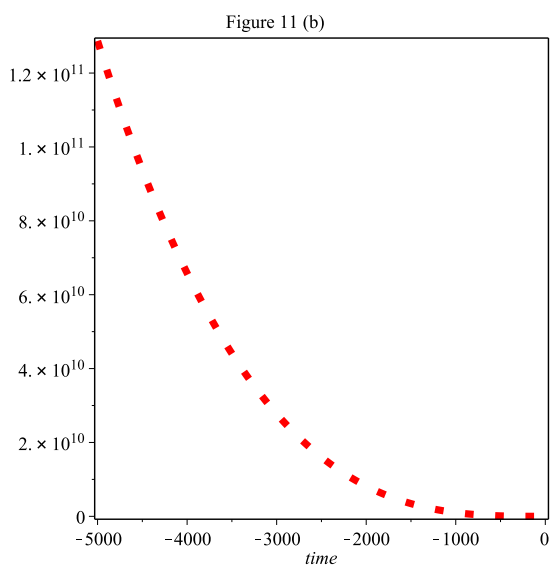
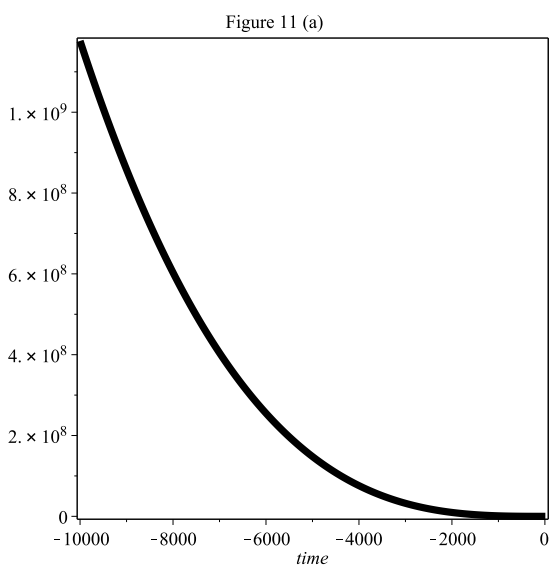
Computing the Adomian polynomials by the algorithm presented in [41], Adomian method leads to the following scheme:

$$\begin{aligned}
 u_{1,0} = 320; \quad u_{1,n+1} &= -\left(b_1 + \frac{b_4 x_3^*}{(\alpha x_1^* + 1)^2}\right) \int_0^t u_{1,n}(t) dt - \frac{b_4 x_1^*}{(\alpha x_1^* + 1)} \int_0^t u_{3,n}(t) dt, \\
 u_{2,0} = 907.25; \quad u_{2,n+1} &= -b_2 \int_0^t u_{2,n}(t) dt + b_6 \int_0^t u_{5,n}(t) dt, \\
 u_{3,0} = 51.7; \quad u_{3,n+1} &= -\gamma \int_0^t u_{3,n}(t) dt + \gamma^2 \int_0^t u_{4,n}(t) dt, \\
 u_{4,0} = 258.5; \quad u_{4,n+1} &= -\gamma \int_0^t u_{4,n}(t) dt + \int_0^t u_{2,n}(t) dt, \\
 u_{5,0} = 79; \quad u_{5,n+1} &= -\gamma \int_0^t u_{5,n}(t) dt + \gamma^2 \int_0^t u_{6,n}(t) dt, \\
 u_{6,0} = 395; \quad u_{3,n+1} &= -\gamma \int_0^t u_{6,n}(t) dt + \int_0^t u_{1,n}(t) dt. \quad (24)
 \end{aligned}$$

The approximate solution of the above system (24), using adomain iterative procedure with two iterations yields:

$$\begin{aligned}
 u_1(t) &= 320 - 2.63345854t + 0.06702425945t^2 - 0.001169678653t^3 + \dots \\
 u_2(t) &= 907.25 - 176.409950t - 18.18786584t^2 - 1.033212645t^3 - \dots \\
 u_3(t) &= 51.7 + 17.111t^2 - 1.061062166t^3 - \dots \\
 u_4(t) &= 258.5 + 855.55t - 5.97533750t^2 + 5.6642266114t^3 - \dots \\
 u_5(t) &= 79 + 4.82t^2 - 0.0175563897t^3 + \dots \\
 u_6(t) &= 395 + 241t - 22.78327077t^2 - 1.496543298t^3 - \dots \quad (25)
 \end{aligned}$$

The above solution (25), is coinciding approximately with the exact solutions of (10). The graphs of $u_1(t), u_3(t), u_3(t), u_4(t), u_5(t)$ and $u_6(t)$ their approximations are shown in figures (11 (a) - 11 (f)).



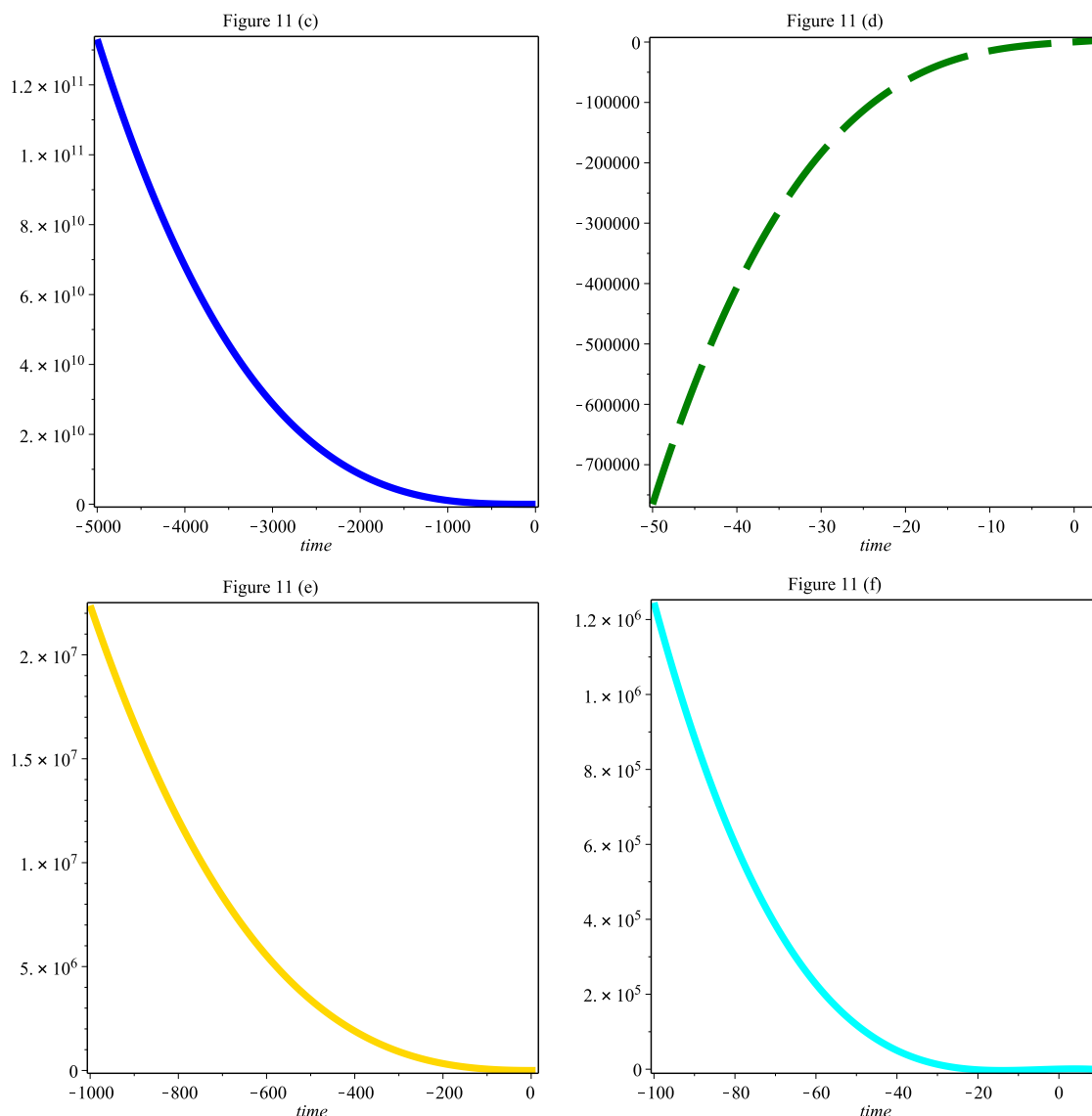


Fig. 11(a)-11(f) shows that the iterative plots for the system (25) with subject data F1.

From the above plots (11 (a) - 11 (f)), we conclude that the system (10) is stable by Adomain decomposition method. Hence, we have verified our system (10) is stable, using our experimental data through analytically and numerically (by Adomain decomposition method).

6 Discussion

This paper was focused on mathematical analysis of glucose-insulin IVGTT model with two distributed delays. A potential application of our study here is to find better ways of delivering insulin and timing of the intake of glucose. Previous studies are largely done on Linear compartment models [42, 43] or on the minimal type models [44]. Our theoretical and numerical findings are showing that in clinic applications. Another possible usage of work is to design effective ways to estimate the involved parameters using sensitivity for

clinic applications.

The Minimal Model has played a crucial role in modeling the glucose-insulin system and it still is of practical use in many clinical settings. Nevertheless, many criticisms have been raised in the last decade. Some questionable physiological assumptions are that the pancreas is able to linearly increase its rate of insulin secretion with time, or the introduction of a non-observable remote compartment to model the insulin effect on the insulin-dependent glucose uptake. The main drawbacks are the lack of mathematical coherence of the model and the lack of robustness in the parameter identification procedure. From a mathematical point of view, it has been proved for that the Minimal Model is not coherent, since it does not admit a steady-state solution (corresponding to the basal glycemia/insulinemia), but allows an unbounded increase of the state variables for a reasonable set of model parameters. This is mainly due to the time-varying term and the values the target glycemia assumes according to data, which are smaller than the measured basal glycemia. This drawback clearly affects the estimate of the insulin sensitivity index also, since it is defined as a steady-state index, but it is estimated by use of a mathematical model which does not admit a steady-state solution. But our described model with using Michaleis-Menton form overcome all the drawbacks of Minimal Model. And it can easily verified from the figures (8-10) and also it converges to the steady state solution.

The sensitivity functions are useful to evaluate which parameters are of a significant uncertainty effect in the glucose and insulin concentration levels. Comparison between $F1$, $R1$ and $R2$ can easily show that the parameters b_6 and b_4 are play crucial role in this model. This was shown in the above Figures. (1(a) – 4(f)).

Pitchaimani *et.al.* [38] considered a two discrete delay for IVGTT model, they showed that in theory, the IVGTT model [6] is best fitting for all existing data. But our model shows that, it satisfies not only the existing data but also the 40 subjects (for the minimum range $R1$ and the maximum range $R2$, the parameters estimate from the WLS Methods) [35].

For this model was fitted on data from each one of the experimental subjects. The test were conducted at a level $\alpha = 0.01$. However, even accurate identification of the parameter value from experimental data would not only to allow analytically but also numerically (for the comparison of observed data) fitted on our model. The availability of real-time data on the insulin concentration is a prerequisite for the development of an artificial pancreas controlling in real time the blood glucose level with optimum insulin infusions.

References

- [1] R.N. BERGMAN, Y.Z. IDER, C.R. BOWDEN, C. COBELLI, Quantitative estimation of insulin sensitivity *Am. J. Physiol.*, 236(6): E667-77, (1979).
- [2] G. TOFFOLO, R.N. BERGMAN, D.T. FINEGOOD, C.R. BOWDEN, C. COBELLI, Quantitative estimation of beta cell sensitivity to glucose in the intact organism: a minimal model of insulin kinetics in the dog, *Diabetes*, 29 (12): 979-90, (1980).
- [3] J. Li, Y. Kuang, B. Li, Analysis of IVGTT glucose - insulin interaction models with time-delay, *Dis. and Contin. Dyn. Syst. - Series B*, 1 (1): 103-124, 2001.

- [4] A. MUKHOPADHYAY, A. DE GAETANO, O. ARINO, Modelling the intra-venous glucose tolerance test: a global study for a single distributed delay model, *Dis. and Contin. Dyn. Syst. - Series B*, 4(2): 407-417, (2004).
- [5] P. PALUMBO, A. DE GAETANO, S. PANUNZI, Qualitative behaviour of family of delay-differential models of the glucose-insulin system, *Istituto Di Analisi Dei Sistemi Ed Informatica Consiglio Nazionale Delle Ricerche*, 7(2): 399. (2007).
- [6] A. DE GAETANO, O. ARINO, Mathematical modelling of the intravenous glucose tolerance test *J. Math. Biol.*, 40(2): 136 - 168, (2000).
- [7] V.W. BOLIE, Coefficients of normal blood glucose regulation, *J. Appl. Physiol.*, 16: 783-788, (1961).
- [8] E. ACKERMAN, L.C. GATEWOOD, J.W. ROSEVEAR, G.D. MOLNAR, Model studies of blood-glucose regulation, *Bull. Math. Biophys.*, 27: Suppl: 21 - Suppl: 3, (1965).
- [9] G. SUBBA RAO, J.S. BAJAJ, J. SUBBA RAO, A mathematical model for insulin kinetics. II. Extension of the model to include response to oral glucose administration and application to insulin-dependent diabetes mellitus (IDDM), *J. Theor. Biol.*, 142: 473-483, (1990).
- [10] R.C. Turner, A.S. Rudenski, D.R. Matthews, J.C. Levy, S.P. O'Rahilly, J.P. Hosker, Application of structural model of glucose-insulin relations to assess beta-cell function and insulin sensitivity, *Horm Metab Res*, 24: 66-71, (1990).
- [11] J. Proietto, Estimation of glucose kinetics following an oral glucose load. Methods and applications, *Horm. Metab. Res.*, 24 : 25-30, (1990).
- [12] M. NOMURA, M. SHICHIRI, R. KAWAMORI, Y. YAMASAKI, N. IWAMA, H. ABE, A mathematical insulin-secretion model and its validation in isolated rat pancreatic islets perfusion, *Comput. Biomed. Res.*, 17: 570-579, (1984).
- [13] W.J. SLUITER, D.W. ERKELENS, P. TERPSTRA, W.D. REITSMA, H. DOORENBOS, Glucose tolerance and insulin release, a mathematical approach. II. Approximation of the peripheral insulin resistance after oral glucose loading, *Diabetes*, 25: 245-249, (1976).
- [14] L.C. GATEWOOD, E. ACKERMAN, J.W. ROSEVEAR, G.D. MOLNAR, T.W. BURNS, Tests of a mathematical model of the blood-glucose regulatory system, *Comput. Biomed. Res.*, 2: 1-14, (1968).
- [15] F. CERESA, F. GHEMI, P.F. MARTINI, P. MARTINO, G. SEGRE, A. VITELLI, Control of blood glucose in normal and in diabetic subjects. Studies by compartmental analysis and digital computer technics, *Diabetes*, 17: 570-578, (1968).
- [16] L. JANSSON, L. LINDSKOG, N.E. NORDEN, Diagnostic value of the oral glucose tolerance test evaluated with a mathematical model, *Comput. Biomed. Res.*, 13: 512-521, (1980).
- [17] M.D. O'CONNOR, H. LANDAHL, G.M. GRODSKY, Comparison of storage and signal-limited models of pancreatic insulin secretion, *Am. J. Physiol.*, 238: R378-R389, (1980).

- [18] J. STURIS , K.S. POLONSKY , E. MOSEKILDE , E. VAN CAUTER, Computer model for mechanisms underlying ultradian oscillations of insulin and glucose, *Am. J. Physiol.*, 260: E801-E809, (1991).
- [19] B. TOPP, K. PROMISLOW, G. DeVRIES, R.M. MIURA, D.T. FINEGOOD, A model of beta-cell mass, insulin, and glucose kinetics: pathways to diabetes, *J. Theor. Biol.*, 206: 605-619, (2000).
- [20] I.M. TOLIC, E. MOSEKILDE, J. STURIS, Modeling the insulin-glucose feedback system: the significance of pulsatile insulin secretion, *J. Theor. Biol.*, 207: 361-375, (2000).
- [21] Y. LENBURY, S. RUKTAMATAKUL, S. AMORNSAMARNKUL, Modeling insulin kinetics: responses to a single oral glucose administration or ambulatory-fed conditions, *Bio. syst.*, 59: 15-25, (2001).
- [22] A. J. L MAKROGLOU, Y. KUANG, Mathematical models and software tools for the glucose-insulin regulatory system and diabetes: an overview, *Appl. Num. Math.* 56: 559 - 573, (2006).
- [23] L. S. G. BENNETT, Asymptotic properties of a delay differential equation model for the interaction of glucose with plasma and interstitial insulin, *Appl. Math. and Comput.*, 151: 189-207, (2004).
- [24] R. PRAGER, P. WALLACE, J.M. OLEFSKY, In vivo kinetics of insulin action on peripheral glucose disposal and hepatic glucose output in normal and obese subjects, *J. Clin. Invest.*, 78: 472-481, (1986).
- [25] E.T. SHAPIRO, H. TILLIL, K.S. POLONSKY, V.S. FANG, A.H. RUBENSTEIN, E. VAN CAUTER, Oscillations in insulin secretion during constant glucose infusion in normal man: relationship to changes in plasma glucose, *J. Clin. Endocrinol. Metab.*, 67: 307-314, (1988).
- [26] G. PACINI, R. N. BERGMAN, MINMOD: a computer program to calculate insulin sensitivity and pancreatic sensitivity from the frequently sampled intravenous glucose tolerance test, *Comput. Methods Programs Biomed.*, 23 (2): 113-122, (1986).
- [27] M. E. FISHER, K. L. TEO, Optimal insulin infusion resulting from a mathematical model of blood glucose dynamics, *IEEE Trans. on Biomed. Eng.*, 36 (4): 479-486, (1989).
- [28] M. E. FISHER, A semiclosed-loop for the control of blood glucose levels in diabetics, *IEEE Trans. on Biomedical Engineering*, 38 (1): 57-61, (1991).
- [29] A. CAUMO, R.N. BERGMAN, C. COBELLI, Insulin sensitivity from meal tolerance tests in normal subjects: a minimal model index, *J. Clin. Endocrinol. Metab.*, 85 (11): 4396-402, (2000).
- [30] G.M. STEIL, A. VOLUND, S.E. KAHN, R.N. BERGMAN, Reduced sample number for calculation of insulin sensitivity and glucose effectiveness from the minimal model, *Diabetes*, 42(2): 250-6, (1993).

- [31] R.N. BERGMAN, C. COBELLI, Minimal modeling / partition analysis and the estimation of insulin sensitivity, *Fed. Proc.*, 39 (1): 110-5, (1980).
- [32] T.A. GRESL, R.J. COLMAN, T.C. HAVIGHURST, L.O. BYERLEY, D.B. ALLISON, D.A. SCHOELLER, J.W. KEMNITZ, Insulin sensitivity and glucose effectiveness from three minimal models: effects of energy restriction and body fat in adult male rhesus monkeys, *Am J. Physiol. Regul. Integr. Comput. Physiol.*, 285 : R1340, (2003).
- [33] A. DE GAETANO, D. DI MARTINO, A. GERMANI, C. MANES, P. PALUMBO, Distributed delay models of the glucose-insulin homeostasis and asymptotic state observation *Istituto Di Analisi Dei Sistemi Ed Informatica Consiglio Nazionale Delle Ricerche*, R.618, (2004).
- [34] D.V.GIANG, Y. LENBURY, A. DE GAETANO, P. PALUMBO, Delay model of glucose insulin systems: global stability and oscillated solutions conditional on delays, *J. Math. Anal. Appl.*, 343(2)-996, (2008).
- [35] S. PANUNZI, P. PALUMBO, A. DE GAETANO, A discrete single delay model for the intravenous glucose tolerance test, *Theor. Biol. Med. Model.*, 35 (4): 1-16, (2007).
- [36] Y. KUANG, Delay Differential Equations with Applications in Population Dynamics, *The Series of Math. in Sci. & Eng.*, 191: Academic Press, Boston. (1993).
- [37] J.K. HALE, J. KATO, Phase space for retarded equation with infinite delay, *Funkcial. Ekvac.*, 21: 1141. (1978) .
- [38] M. PITCHAIMANI, P. KRISHNAPRIYA, C. MONICA, Mathematical modeling of intravenous glucose tolerance test model with two discrete delays, *J. Biol. Syst.*, 23 (4) : 631-660, (2015).
- [39] XIAOXIN LIAO, LIQIU WANG, PEI YU, Stability of Dynamical Systems, 1st ed., Elsevier, (2007).
- [40] F.A. RIHAN, Sensitivity analysis of dynamical systems with time lags, *J. Comput. Appl. Math.*, 151, 445-463, (2003).
- [41] J. BIAZAR, E. BABOLIAN, A. NOURI, R. ISLAM, An alternate algorithm for computing Adomian decomposition method in special cases, *Appl. Math. Comput.*, 138, 1-7, (2003).
- [42] G.W. SWAN, An optimal control model of diabetes mellitus, *Bull. Math. Biol.*, 44: 793-808, (1982).
- [43] G.W. SWAN, Applications of Optimal control theory in biomedicine, Marcel Dekker, NewYork, (1984).
- [44] M. E. FISHER, A semiclosed-loop algorithm for the control of blood glucose levels in diabetics, *IEEE. Tran. Bio. Eng.*, 38: 57-61, (1991).